Structure and properties of selected metal organic frameworks as adsorbent materials for edible oil purification

E. Yılmaz*
A. Erden
M. Güner

Çanakkale Onsekiz Mart University,
Faculty of Engineering, Department of
Food Engineering
Çanakkale, Turkey

The scope of this study was to evaluate adsorbent material properties of some selected metal organic frameworks (MOFs) in comparison with natural clays (commercial bleaching earth-C.B.E., natural zeolite and sepiolite) for possible applications in edible oil purification. Seven MOFs were synthesised at gram level in the laboratory and the 3 clays were acid activated. Microstructural properties by scanning electrone miscoscopy (SEM), crystallinity properties by X-ray diffraction (X-RD), surface and pore properties by BET analysis, some spectral properties (NIR and 1H NMR), thermal properties by differential scanning calorimetry (DSC), and some adsorption properties were determined. It was shown that the synthesized MOFs represent morphologies like sphres, needles, cubic crystals, and amorphous masses. Their X-RD patterns indicated occurrence of different crystalline types. The largest surface area in aluminum-MOF (Al-MOF) and ZIF-8-MOF, largest pore volume in sepiolite and titanium-MOF (Ti-MOF), and largest pore radius in gamma-cyclodextrine-MOF (γ-CD-MOF) were measured. Near infrared (NIR) and nuclear magnetic resonance (1H NMR) spectroscopy proved that coordination structures with metal nuclei and surrounding hydrogens were present. Thermal analysis indicated that except γ-CD-MOF, all adsorbents were quite heat stable up to 450°C temperatures. Finally, higher free fatty acid adsorption capacities in Ti-MOF, γ-CD-MOF, Cr-MOF, and higher β-carotene adsorption capacities in Ti-MOF and γ-CD-MOF were measured. This study proved the great potential of the MOFs as adsorbents for various purification purposes in the edible oil industry.

Keywords: metal organic fameworks; adsorbent; property; oil; purification.

(*) CORRESPONDING AUTHOR:
Prof. Dr. Emin YILMAZ
Tel: +90286-2180018 / 2170
Fax: +90 286 2180541
E-mail: eyilmaz@comu.edu.tr

INTRODUCTION

Metal Organic Frameworks (MOF) or coordination polymers are defined as the materials constructed by joining metal-containing units with organic linkers through strong bonds by reticular synthesis to create open crystalline frameworks with permanent porosity and aesthetically interesting structures. These structures pose huge porosity, regular cavities, dynamic flexibility, and others. Hence, MOFs are very suitable materials for gas adsorption and storage, separation, sensors, analysis, luminescence, magnetism, drug delivery, and selective adsorption applications [1, 2, 3]. Transition metals, alkaline earth elements, *p*-block elements, actinides and mix metals have been used [4] in MOF synthesis with various organic linkers (ligands) such as terephthalic acid, formic acid, oxalic acid, adipic acid, 1,3,5-benzenetribenzoic acid, 2,2-bis(1,3-dithiolylidene)-tetrayl-tetrabenzoate, 2-methylimidazole, catenane, mixed-linker compounds and others [1, 2, 4, 5]. Synthesis of MOFs is usually based on liquid-phase syntheses, where metals and ligands are solubilized in a suitable solvent based on its reactivity, solubility, redox potential, stability, availability, and price. Generally, reactions take place in closed vessels above boiling point

of solvent and under autogeneous pressure. Although synthesis in laboratory scale is straightforward, during scaling-up some safety issues arise. With countless technical variations, usual MOF syntheses are based on solvothermal, microwave-assisted, electrochemical, mechanochemical, and sonochemical syntheses techniques. Also, some postsynthesis modifications could be possible. Hence, depending on the selection of metals and linkers, and method and conditions of synthesis (molar ratios of starting materials, solvent type, pH, reaction temperature and time, pressure, presence of additional linkers, modifications etc.) many different topologies of MOFs could be designed [1, 2, 4]. It was stated that MOFs are already beyond the status of laboratory curiosity for various applications, and feasibility of large-scale synthesis demands cost and safety at first [5]. Not to mention other applications, usage of MOFs in food sector is very new. It was indicated that Basosiv M050 was used as gas scavanger inside bananas packaging, and longer shelf-life of fruit due to ethylene adsorption was encountered [5]. It was stated that γ-cyclodextrine based MOFs are safe and even edible and could be used directly in foods [6].

The MOF, MIL-101 was used to selectively adsorp and remove (diversive micro-solid-phase extraction) herbicides from soy, sunflower, corn, and peanut oils. The triazine and phenylurea herbicides were recovered by 87.3-107%, respectively [7]. The first and only study [8] reporting the application of MOFs in edible vegetable oil purification is accomplished with MIL-53 (Al), Zn-MOF and MIL-125 (Ti) samples. It was shown that these MOFs improve physicochemical properties of unrefined vegetable oils by binding free acids and peroxides. The results of this study clearly pointed out that different MOFs could be synthesized and used in edible oil industries for different purposes.

It is well known that porous materials or adsorbents have been used in vegetable oil bleaching [9], decolorization [10], physical refining [11], stabilization [12], extention of frying oil shelf-life [13] and similar purposes. Natural montmorollonites and zeolites, active carbon, diatomaceous earth, silicates, celite, charcoal, fuller's earth, and various commercial bleaching clays have been used in vegetable oil industry [14]. Depending on oil material properties and selected process criteria, around 1.0-3.0% clay addition and heating around 75-110°C is applied for around half an hour to realise the adsorption principle to remove the pigments and other impurities (free fatty acids, peroxides, phospholipids, Maillard products, metals, etc.) from the oils [9,14].

In this study, we selected seven different MOFs based on their safety knowledge and synthesised them at gram level in our laboratory with known synthesis reactions indicated in literature. Furthermore, three different natural adsorbents (commercial bleaching earth, natural zeolite and sepiolite) were selected for comparison purposes. The objective of the current study was to evaluate these ten different materials for possible applications in edible oil purifications. Hence, the morphology and microstructure (scanning electrone microscopy images and X-ray diffraction patterns), surface and pore properties (using Brunauer-Emmett-Teller-BET equation), spectral properties (near infraredspectroscopy-NIR and nuclear magnetic resonance spectroscopy-NMR), thermal properties (differential thermal calorimetry-DSC), and oil purification properties (free fatty acid and β-carotene adsorption capacities) for the adsorbents were determined and compared. Although Vlasova et al. [8] used three different MOFs in vegetable oil purification, this study is rather focused on the evaluation of the possibility of using seven different and synthesized MOFs as adsorbenst materials for various edible oil purification applications through measurements of their structure/pore properties and adsorption capacities in details.

EXPERIMENTAL

MATERIALS

All chemicals and solvents used in this study, such as terephthalic asit, γ-cyclodextrine, potassium hydroxite, crome-3-nitrate nonahydrate, hydrofluoric acid, aluminium chloride, aluminium nitrate nonahydrate, acetic acid, nitric acid, 2,5-furandicarboxylic acid, magnezium nitrate, zinc nitrate hexahydrate, 1,4-benzene dicarboxylic acid, 2-methylimidazole, titanium (IV) butoxide, N,N-dimethylformamide, acetone, methanol, ethanol, chloroform and others were purchased from Merck (Darmstadt, Germany), Sigma-Aldrich (St. Louis, USA), Acros organics (New Jersey, USA), and Abcr (Karlsruhe, Germany). Beta-carotene (30% oil suspension) was purchased from Allied Biotech Corp. (Taipei, Taiwan). Commercial bleaching earth by Trakya Birlik Oil Processing Factory (Çorlu, Tekirdağ), natural zeolite by Rota Mines Co. (İstanbul), and natural sepiolite by Madkim Coal and Chem. Co. (İstanbul) were gifted. All other utensils were purchased from local stores.

SYNTHESES OF THE METAL ORGANIC FRAMEWORKS

The titanium-MOF (Ti-MOF) was synthesised following the method [8]. Briefly, 16,6 g terephthalic acid was dissolved in 300 mL dimethylformamide, and after the addition of 17 g titanium butoxide, the mixture refluxed for 6 h. After cooling, the crystals were filtered and washed with dimethylformamide and acetone successively, before drying at 190°C under vacuum. Finally, it was placed into coloured glasses and was desiccated during the analysis. Under the same conditions, several syntheses were completed

to collect enough amount (around 100 g) of MOF for this study. The same procedure was followed for all MOFs synthesised in this study.

Gamma-cyclodextrine-MOF (γ-CD-MOF) was synthesised according to [15] 1.30 g γ-cyclodextrine and 0.45 g potassium hydroxide were dissolved in 20 mL deionised water and stirred at 500 rpm until dissolution. Then, the solution was filtered and and put in a beaker with 50 mL methanol and sealed. The beaker was stored at 23 ± 0.1°C and 50 ± 2% relative humudity for 7 days. Finally, the formed crystals were filtered, and washed with 30 mL of methanol for 3 times before drying them 10 h at 25°C under vacuum and 12 h at 45°C. After cooling to room temperature, the MOF crystals were put into coloured glasses.

Crome nitrate-MOF (Cr-MOF) was synthesised by modifying the procedure of [7]. Briefly, 800 mg $Cr(NO_3)_3.9H_2O$, 322 mg terephthalic acid, 0.1 mL hydrofluoric acid were mixed in 9.6 mL ultrapure water, and sealed in a Teflon autoclave. The autoclave was placed in an oven set 220°C for 8 h. After cooling the autoclave, the green colored crystals were washed several times with dimethyl formamide and ethanol. Finally, it was dried at 150°C in an oven for 12 h, before placing into colored and closed glasses.

Aluminium-MOF (Al-MOF) was synthesized according to [3] with some modifications. 4.98 g terephthalic acid, 3.0 g $AlCl_3$ and 6 mL acetic acid were dissolved in 120 mL dimethyl formamide until the solution became transparent. Then, the solution was placed in Teflon autoclave, sealed and heated at 190°C for 72 h. Finally, the autoclave was cooled to room temperature, opened, and solid crystals were washed thoroughly with dimethyl formamide, bofere drying it at 180°C for 2 days in a vacuum oven. The synthesised MOF was placed into colored glasses and kept desiccated during the analysis.

Zinc nitrate-MOF (Zn-MOF) was synthesised by solvothermal reaction [16]. In 100 mL dimethyl formamide and 100 mL methanol, 1.93 g 2,5-furandicarboxylic acid and 3.7 g $Zn(NO_3)_2.6H_2O$ were dissolved. The solution was incubated at 120°C for 3 days in an oven. Finally, the solids were filtered and washed with methanol several times, before drying at 180°C for 2 days under vacuum. Finally, stored in the same way.

Magnesium-MOF (Mg-MOF) was synthesised by following modified technique of [17]. 14 g $Mg(NO_3)_2.6H_2O$ and 280 mL dimethyl formamide were mixed and incubated at 130°C for 5 days in a tightly colosed beaker. The solids, then filtered, washed with dimethyl formamide and methanol, and dried at 180°C for 2 days in the same way.

Zeolitic zinc-MOF (ZIF-8-MOF) was synthesised following [18]. Briefly, 0.21 g $Zn(NO_3)_2.4H_2O$ and 0.06 g 2-methylimidazole were dissolved in 18 mL dimethyl formamide. In a programmed oven, the mixture was heated to 140°C by 5°C/min rate. Then, the solids were decanted from the liquid, and 20 mL of chloroform was added and mixed. Finally, the crystals were fitered and washed with dimethylformamide three times, before drying under air flow at ambient temperature for 2 days. Lastly, stored in the same way as others.

The MOF synthesis techniques are summarised in Table I for an overall visualization and comparison.

ACID ACTIVATION OF THE NATURAL ADSORBENTS

While commercial bleaching earth was already preactivated, and not activated in this study, the other two natural adsorbents, natural zeolite and sepiolite were acid activated. Each adsorbent was mixed with 0.1 M nitric acid (1:10, w/v), and heated (60°C) and stirred (240 rpm) on a heating magnetic stirrer under an hood for 4 h. Then, they are filtered and washed with pure water until the pH of filtrate becomes 6.0. Finally, activated adsorbents were dried in an oven at 110°C to full dryness.

The seven synthesised MOFs and 3 selected natu-

Table I - The techniques used to synthesize the MOFs

MOF	Metal Core / Ligand	Method of Synthesis	Ref.
Ti-MOF	$Ti(OCH_2CH_2CH_2CH_3)_4$ / Terephthalic acid	Solvothermal: N,N-dimethylformamide solvent, reflux at 190°C, 6 hours	[8]
γ-CD-MOF	γ-Cyclodextrine / KOH	Vapour diffusion: Methanol solvent, 23 ± 0.1°C, 50 ± 2% RH, 7 days	[15]
Cr-MOF	$Cr(NO_3)_3.9H_2O$ / Terephthalic acid + Hydroflouric acid	Solvothermal: Ultrapure water, 220°C, 8 hours	[7]
Al-MOF	$AlCl_3$ / Terephthalic acid + Acetic acid	Solvothermal: N,N-dimethylformamide solvent, 190°C, 72 hours	[3]
Zn-MOF	$Zn(NO_3)_2.6H_2O$ / 2,5-Furandicarboxylic acid	Solvothermal: N,N-dimethylformamide + Methanol solvent, 120°C, 3 days	[16]
Mg-MOF	$Mg(NO_3)_2.6H_2O$ / N,N-dimethylformamide	Solvothermal: 130°C, 5 days	[17]
ZIF-8-MOF	$Zn(NO_3)_2.4H_2O$ / 2-Methylimidazole	Solvothermal: N,N-dimethylformamide solvent, 140°C by 5°C/min rate, 25 hours	[18]

ral adsorbents used in this study were shown in Figure 1. Throughout this manuscript, the MOFs were named with the short names given in the brackelets above.

Figure 1 - The MOFs and natural clays used as the adsorbent materials.

MORPHOLOGY AND MICROSTRUCTURE

Scanning electron microscopy (SEM) images of all adsorbents (the MOFs and natural clays) were gathered using a JSM-7100F (JEOL, Japan) scanning electron microscope. The samples were placed on a specimen holder carbon band with double-sided scotch tape and coated with Au-Pd (80-20%) under 0.8 mbar/Pa vacuum and 10 mA voltages in a Quorum coating device. Finally, each sample was viewed under microscope at an accelerating voltage of 15 kV and 150-15000 fold magnifications [19].
The X-ray diffraction (X-RD) patterns of the samples were determined with PANalytical Empyrean model (The Netherlands) X-ray diffractometer. Radiation at a scanning rate of 0.02/0.6 (sec) within 4-40° range under 40 kV and 40 mA CuKa (λ = 0.1546 nm) was applied [20].

SURFACE AREA AND PORE VOLUME

Quantachrome Nova 4000E (Quantachrome Instruments, Boynton Beach, FL, US) with nitogen gas, and the Brunauer-Emmett-Teller (BET) and Langmuir methods were used to determine the surface area, pore radius and pore volume of the adsorbent materials. To determine the surface area, 0.01-2.000 m^2/g range, and to determine pore radius, 3.5-2000 Å range was used [15].

SPECTRAL PROPERTIES

NIR spectra of the adsorbent samples were collected by using FT-NIR Nicolet IS50 Flex Gold infrared spectrometer (Thermo Fisher Scientific, Madison, WI, USA) in diffuse reflectance mode. The unit was equipped with a Germanium coated Potassium bromide (KBr) beam splitter (11000-375 cm^{-1}) and Indium Gallium Arsenide detector. First, the samples were equilibrated at 25 ± 2°C. 5 g of each sample was placed into a petri dish ensuring a full coverage and was gently pressed to degas. The spectral range of 10000-4000 cm^{-1} with 4 cm^{-1} resolution was applied for sample spectra collection. Interferograms of 64 scans were co-added during each spectrum collection to improve the noise signal. Also, a background spectrum was acquired before measurements to account for environmental variations. A cup spinner apparatus was used for measurements to count for any non-homogeneity. Duplicate independent spectral measurements were taken, averaged for each sample and then recorded using Omnic 9 software (Thermo Fisher Scientific, Madison, WI, USA). Finally, the second derivative transformation of the collected spectra (Savitzky–Golay second order polynomial filter with a 25-point window) was completed with multiple variable analysis program Pirouette 4.5 (Infometrix, Inc., Bothell, WA, USA) [21].
Solid-state NMR measurements were recorded on a JEOL ECX 400 (Tokyo, Japan) spectrometer (field strength; MHz) with CP/MAS unit at room temperature and the spinning rate kept at 6 kHz on all samples.

THERMAL PROPERTIES

Thermal behaviour of the adsorbents was assessed with a Perkin-Elmer 400 Differential Scanning Calorimeter-DSC (Gorinstein, The Netherlands) equipped with Pyris 1 Manager Software. Around 5-6 mg sample was weighed and sealed into alumunium pans and placed into sample holder. First, 30 ml/min nitrogen was flushed at 30°C for 10 min, and then the samples were heated from 30 to 450°C by 10°C /min heating rate. The instrument was previously calibrated with Indium and Zinc, and empty pan was used as the reference for duplicate measurements. The DSC thermograms of the adsorbent materials are shown in Figure 2.

FREE FATTY ACID AND β-CAROTENE ADSORPTION CAPACITY

Free fatty acid adsorption capacity of the adsorbents was measured by the method [22]. First, 0.05 M oleic acid solution in hexane was prepared as the stock solution. Then, 0.5 g of each adsorbent and 25 mL of oleic acid solution was mixed and agitated at 150 rpm for 30 min at room temperature. After waiting 20 min for equilibrium, the adsorbent was filtered. Finally, 10 mL ethanol was added to 10 mL of the filtrate and with phenolphthalein indicator, titrated with 0.05 M NaOH solution. The same procedure was done for

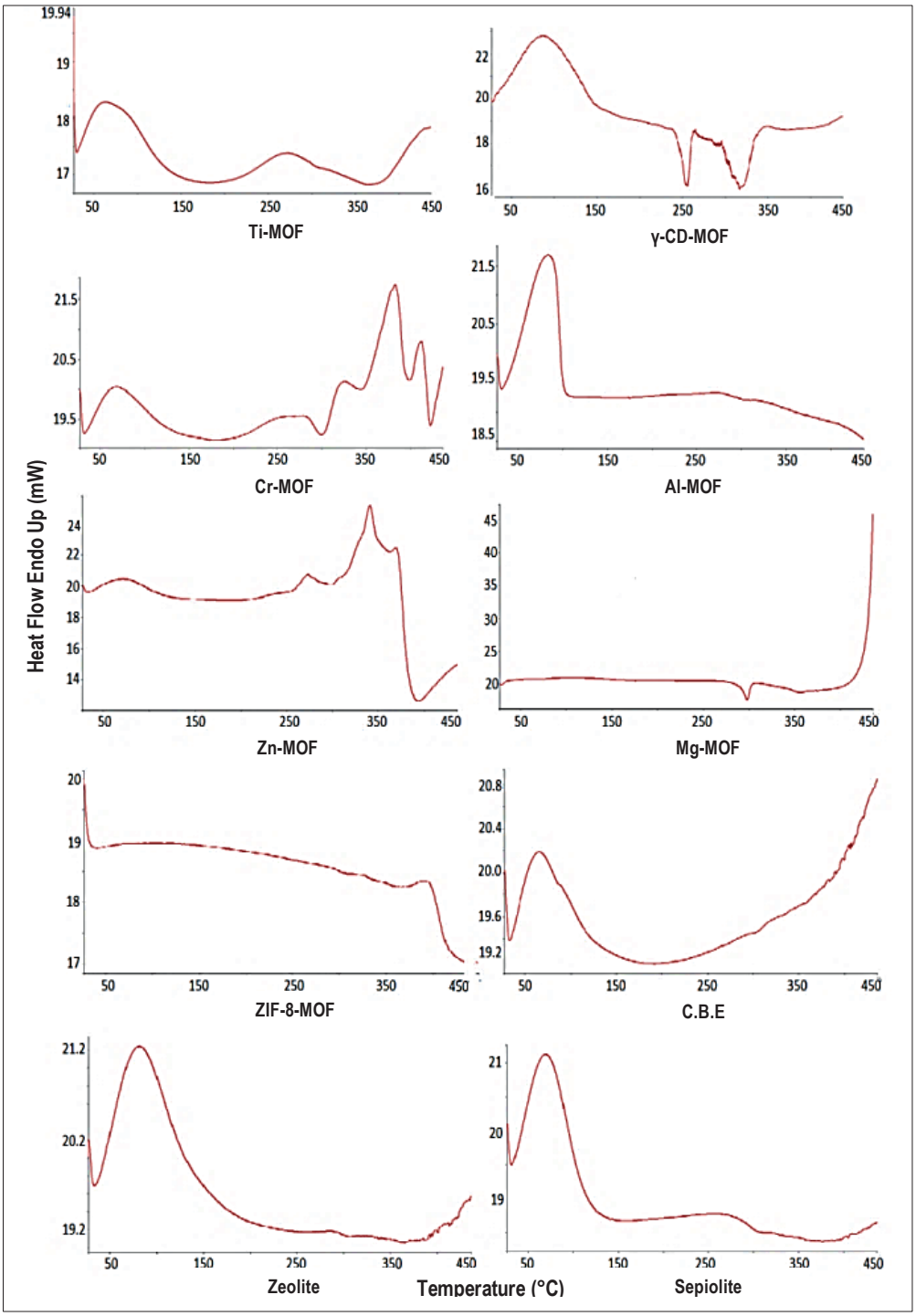

Figure 2 – The DSC thermograms of the MOFs and natural clays

the blank sample, and then adsorption capacity was calculated from the differences of the oleic acid concentrations.

In a similar procedure, β-carotene adsorption capacity was measured. First, 0.5 g β-carotene was dissolved in 500 mL of petroleum ether: aceton (1:1, v/v) as the stock solution. Then, into 20 mL of the stock solution, each of the adsorbents was added at 0.5 g level and mixed for 30 min at room temperature and remained for 30 min for equilibrium. After filtration, the absorbance of the filtrate was recorded at 445 nm (Afilent 8453 UV-Vis Spectrophotometer) against blank (petroleum ether: aceton mixture solvent). The adsorption coefficient of 2592 for β-carotene was used to calculate the remaining β-carotene in the filtrate with the equation given below [23]. From the concentration difference, β-carotene adsorption capacity of each adsorbents was calculated.

$X = A \times Y \times 10^6 / A^{\%}_{1cm} \times 1000$ g

where,

X = amount of β-carotene (μg/100 g)

A = Absorbans value at 445 nm

Y = Amount of the solution (1 mL)

$A^{\%}_{1cm}$ = Absorption coefficient of β-carotene (2592)

STATISTICAL ANALYSIS

The production of each MOF adsorbents was repeated twice. All analyses for the synthesised MOFs and selected natural clays for each repetation were completed at least twice. The results were given as mean values with standard deviation. Comparison of the adsorbents for all measured properties was determined by one-way ANOVA and Tukey's tests with Minitab [24] and SPSS [25] programs. The level of confidence was at least 95% for all statistics.

3. RESULTS AND DISCUSSION

MORPHOLOGY AND MICROSTRUCTURE OF THE ADSORBENTS

The scanning electrone microscopy (SEM) images of the 7 synthesised MOFs and 3 natural clays were presented in Figure 3.

Clearly, quite different crystalline morphologies were observed. Most importantly, these images prove that the coordination polymers formed between the metals and the linkers successfully. As could be observed, Ti-MOF as clustered spheres, γ-CD-MOF as amorphous mass, Cr-MOF as rectangular crystals, Al-MOF as needle like crystals, Zn-MOF as balls, Mg-MOF as mixed geometrical crystals, ZIF-8-MOF as cubic crystals were formed. The structures of the commercial bleaching earth (C.B.E.), sepiolite and zeolite were similar and amorphous. In the study of [3], the SEM image of Al-MOF was quite like the one in this study. Furhermore, different morphologies from spherical balls to rods with several other MOFs were presented in [26]. Also, the image of HKUST-1 MOF was published [27]. As not the same MOF images were published, it could not be possible to compare. Hence, this study provides an important contribution to the literature for further comparisons and evaluations.

It was stated that the synthesis conditions and post-synthesis modification could affect the morphology of any MOF [28, 29]. It was also stated that if metal concentration is high during synthesis, larger crystals are formed. Furthermore, types of ligands (mono or poly-toothed) affect MOF structure and crystalline size [28]. Likewise, it was stated that if the ligand concentration is high, lesser nucleation occurs and larger crystals forms [29]. One study [30] showed that in the presence of pyridine, short hexagonal crystals, while in the absense of pyridine, longer hexagonal rod crystals were formed. In this study, we followed the above explained synthesis conditions and generated the observed MOF morphologies.

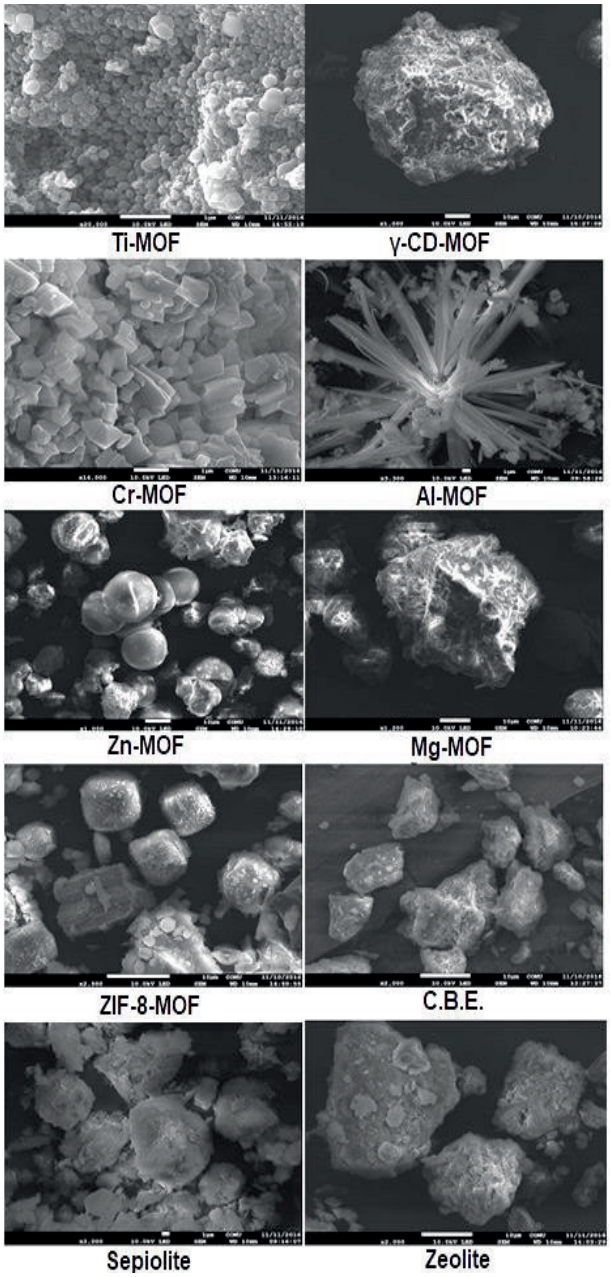

Figure 3 - The scanning electrone microscopy (SEM) images of the MOFs and natural clays

The X-ray diffraction (X-RD) patterns of the adsorbents were presented in Figure 4.

The Ti-MOF had a major peak at 4-6° with high intensity. The same peak was observed in [8] for the Ti-MOF, which we followed their synthesis method. Furthermore, peaks at around 11 and 18° were ap-

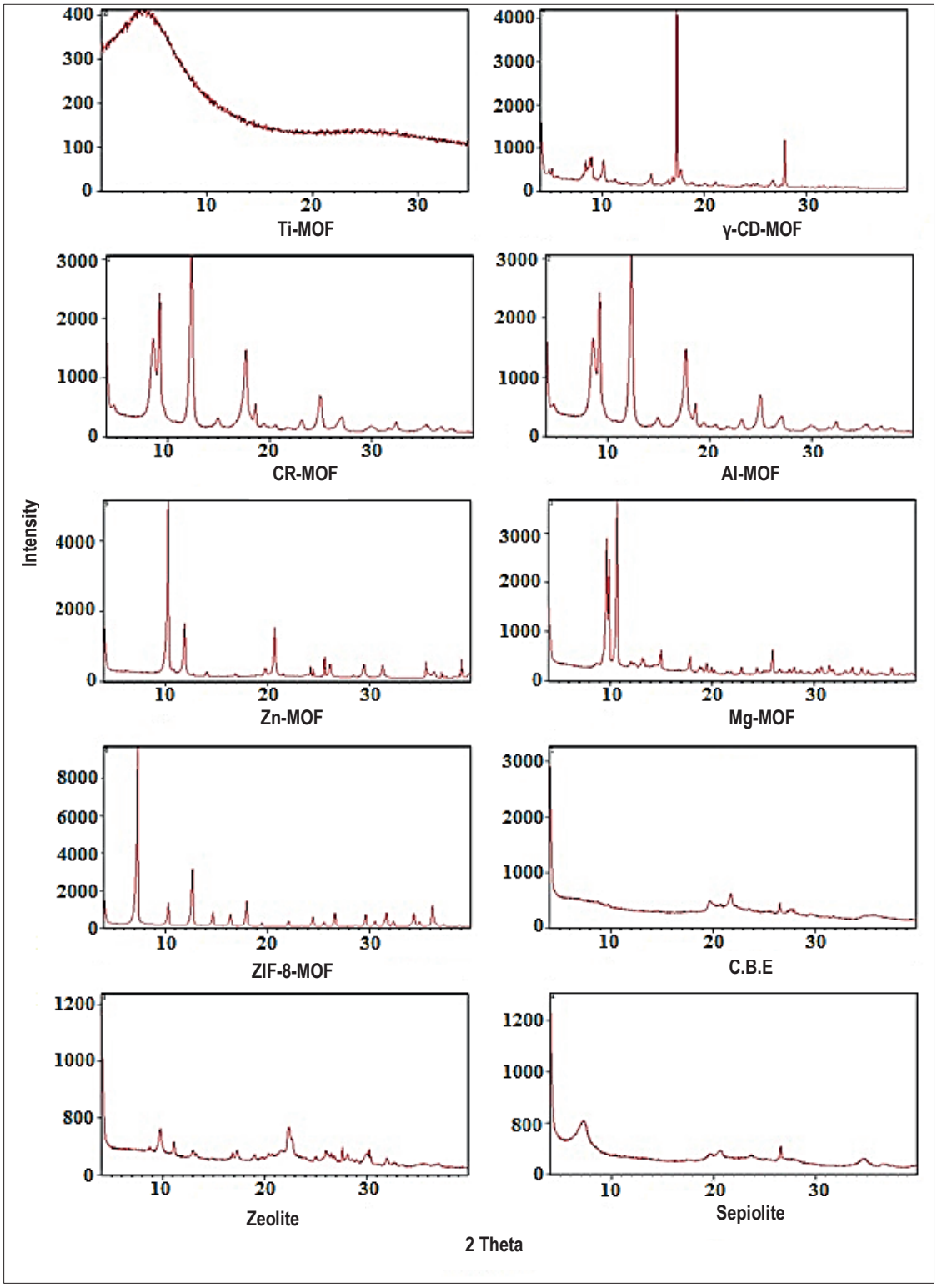

Figure 4 - The X-ray diffraction (X-RD) patterns of the MOFs and natural clays

parent in theirs, but not visible in our sample. Because the intensity of the peak at 4-6° is so large, it was not possible to observe the other two peaks, although they were present in lesser intensities. This difference might be caused due to synthesis conditions or difference in the materials used. Hence, true crystalline forms of Ti-MOF were gained. The X-RD patterns of γ-CD-MOFs synthesised by [6,15] were published. They observed one peak at 4°, 3 peaks at around 5-10°, one peak at 17-18° and one peak at around 23-25°. As could be observed from Figure 4, very similar peaks were in the synthesised γ-CD-MOF in this study. Hence, very similar crystal types were formed. Almost the same X-RD patterns of the

synthesised Cr-MOF was observed in the study of [7]. Clearly, peaks at around 3, 5, 6, 9, 10, and 17° were present in both studies, indicating the same crystalline structures. The X-RD patterns of Al-MOF was also published [3]. Peaks at around 8-10°, 16° ve 18° were observed both in [3], and in this study. The X-RD patterns of Ti-MOF, Al-MOF and Zn-MOF published in [8] were quite like those presented in this study. The data presented in [18] for ZIF-8-MOF is almost the same with this study. Furthermore, the X-RD patterns of C.B.E., natural zeolite and sepiolite indicate that there were some crystallinity present, but not as much as in the MOFs. Hence, these natural clays are mostly made up of an amorphous mass with some crystallinity also as evidenced from the SEM images (Fig. 2). All these results indicate that the desired crystalline forms were developed in the MOF syntheses procedures that followed.

SURFACE AREA AND PORE VOLUME OF THE ADSORBENTS

The surface and pore properties of the adsorbents were presented in Table II. The largest surface area was measured in Al-MOF (1323.67 m^2/g) followed by ZIF-8-MOF (1039.09 m^2/g), while the lowest value was with Zn-MOF (0.86 m^2/g) followed by γ-CD-MOF (1.18 m^2/g). Clearly there is a great variation among the adsorbents prepared. Although not as much as in the surface areas, there was some significant differences among the adsorbents for their pore volume values (Tab. II).

The highest pore volume was measured in sepiolite (0.93 cm^3/g), while the lowest value was in Zn-MOF (0.01 cm^3/g). Generally, it could be said that Zn-MOF seems less proper as adsorbent with its lower surface area and pore volume. It might be caused from materials used or synthesis processes applied. The pore radius values of the samples were also varied from the highest of 23.75 nm in γ-CD-MOF sample to the lowest of 1.69 nm in ZIF-8-MOF sample. In the study of Vlasova et al. [8], the surface areas and pore volumes of the Al-MOF, Zn-MOF and Ti-MOF was reported as 1196, 380 and 1310 m^2/g, and 0.76, 0.29 and 0.97 cm^3/gr, respectively. Clearly, Zn-MOF was totally different in this study, while values of Al-MOF was rather similar. Ti-MOF in this study synthesised with the same method [8] had lower surface area and pore volume values. In another study [27], two MOFs synthesised from KNiFC. Surface area values of 47.74 and 111.7 m^2/gr, and pore volume values of 0.13 and 0.25 cm^3/gr were measured. Generally, surface area and pore properties of MOFs seems quite dependent on its metal and ligand type as well as synthesis conditions and post-synthesis modifications applied. Hence, variations have been appreciated as expected results. Values reported in this study are also the first data for literature for the studied MOFs, and hence; would be very valuable for other researchers.

SPECTRAL PROPERTIES OF THE ADSORBENTS

Infrared spectroscopy is a technique based on the interactions of materials with electromagnetic spectrum between 12.800 and 10 cm^{-1} wave number or 0.78 and 1000 μm wavelenght. Techniques of near infrared (NIR), middle infrared (MIR) and far infrared (FIR) were developed based on working range of the spectrum. This spectroscopy is very good for determination of different organic substances within a matrix; hence widely used for foods to determine its components [31]. In this study, NIR at 770-3000 μm wavelenghts or 13.000-3.300 cm^{-1} wave numbers were utilised. At this region, the vibrations of C-H, N-H and O-H bonds would be determined. Hence, it could be used to determine water, phenol, alcohol, organic acid, ester, keton and carboxylic acid moieties. Especially in solid foods, it yields very reliable results for starch, fat, protein, moisture and cellulose components analyses [31]. In the MOF samples, strong bands at 4000-4500 cm^{-1}, 5500-6000 cm^{-1} and 7000-7300 cm^{-1}

Table II - The surface and pore properties of the MOFs and natural clays

	Surface Area (m^2/g)	Pore Volume (cm^3/gr)	Pore Radius (nm)
Ti-MOF	39.03±1.95^{g*}	0.79±0.01^{b}	18.38±0.90^{c}
γ-CD-MOF	1.18±0.05^{h}	0.30±0.01^{f}	23.75±0.10^{a}
Cr-MOF	300.73±15.03^{c}	0.38±0.00^{d}	5.12±0.04^{e}
Al-MOF	1323.67±66.18^{a}	0.67±0.01^{c}	2.04±0.00^{f}
Zn-MOF	0.86±0.04^{h}	0.01±0.01^{f}	20.29±0.01^{b}
Mg-MOF	115.12±5.75^{f}	0.09±0.00^{f}	3.47±0.00^{f}
ZIF-8-MOF	1039.09±51.95^{b}	0.44±0.00^{d}	1.69±0.01^{g}
C.B.E.	146.30±7.31^{e}	0.37±0.01^{d}	10.18±0.00^{d}
Zeolite	179.63±8.98^{d}	0.26±0.01^{e}	5.88±0.00^{e}
Sepiolite	319.92±15.99^{c}	0.93±0.00^{a}	11.62±0.00^{d}

*Small uppercase letters in the same columns show statistically significant differences among the adsorbent materials ($p \leq 0.05$).

wave numbers were observed (Fig. 5).
There is very limited number of studies regarding NIR spectroscopy for MOFs. Wang et al. [32] obtained NIR spectrum of the lanthanide-based MOFs they synthesised. They stated that the ligand, furan-2,5-dicarboxylic acid, yielded single emission band at 396 nm, while the MOFs yielded strong emission peaks at around 891, 1062 and 1331 nm wavelenghts. In another study [27] FT-IR measurements for magnetic seperation of Cs^+ from aqueous solutions with MOF usage were done. It was concluded that Arc-H band showed the presence of aromatic compounds and vibrations of –OH indicated water presence on the MOFs. Lastly, different spectra of some ZIF-8 and HKUST-1 MOFs were taken [33]. Their FT-IR spectra indicated that there are strong emission peaks at around 1700-1300 cm^{-1} and 700 cm^{-1} wave numbers. Overall, the strong peaks shown in Figure 5 for the MOFs synthesised in this study show that different bondings were occurred between the metal cores and the ligands used to form the crystalline MOF structures. These findings are also in accordance with the SEM images (Fig. 3) indicating that the MOFs were formed with diverse topographic structures.
The solid-state nuclear magnetic resonance (SS-NMR) of MOF samples were also obtained and the spectra is presented in Figure 6.
Solid-state NMR spectroscopy uses 4-600 mHz frequency of the electromagnetic spectrum. It is based on the measurement of energy emitted from atom nuclei at the electromagnetic field. Both organic and inorganic materials could be quantified, and their structure can be evaluated by this technique [31]. SS-NMR can probe short range ordering and local structure around the nucleus of interest. Hence, it can provide structural information and host-guest interaction within a MOF. Furthermore, it could be used to confirm the identity of the organic linkers and presence of key functional groups. The powder patterns of MOFs could be evaluated by SS-NMR as well [34].

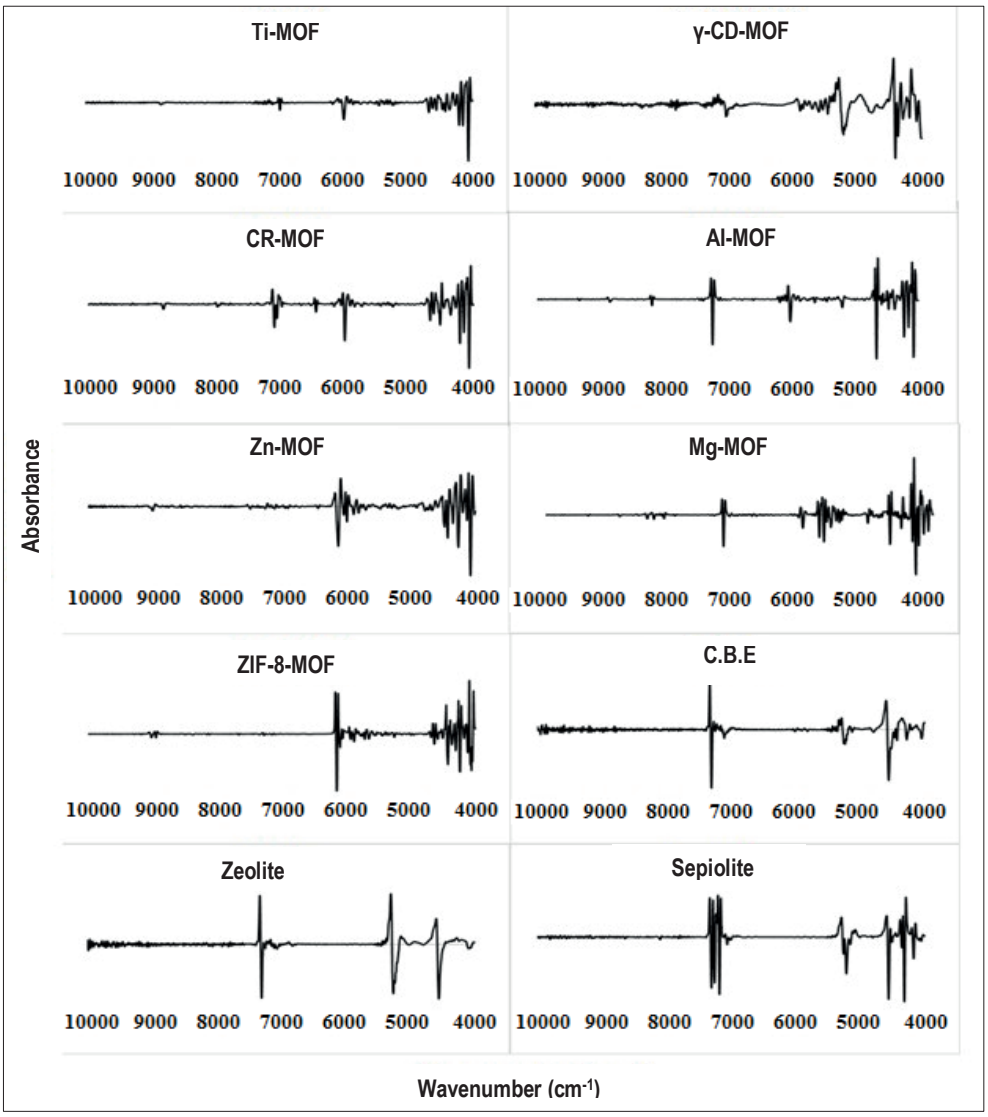

Figure 5 - The near infrared (NIR) spectra of the MOFs and natural clays

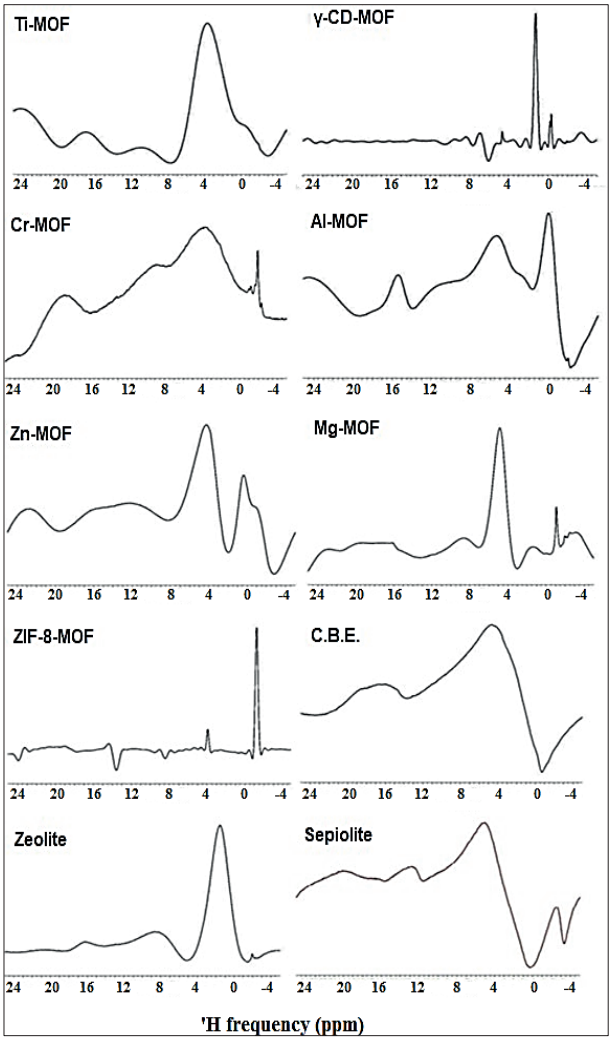

Figure 6 - The ^{1}H NMR spectra of the MOFs and natural clays

It was stated that X-ray diffraction patterns could be good enough to determine the structure of MOFs, but to determine post-synthesis modifications, effects of other functional groups additions and of thermal treatments on MOF structure could only be possible by SS-NMR or similar techniques [35]. In this study, since no post-synthesis modifications or other group additions were done, the purpose was only to determine structural information or identity of the linkers for the synthesised MOFs, and only ^{1}H NMR was studied. In one study [36] Al containing MIL-110 MOF was evaluated with Al and ^{1}H NMR. The NMR spectra indicated presence of clusters of Al skeleton at 0 ppm frequency, and signals of frame work protons (inorganic hydroxyls and aromatic trimesate) and protons of guest molecules such as water trapped within the tunnels at around 5.0 ppm frequency. Similar peaks at the frequency line could be observed in Figure 6 for Al-MOF synthesised in this study. In another similar study [37], ^{1}H NMR spectra of MIL-53 MOF, which is an aluminum terephthalate, was provided. The three signals at 2.9, 7.2, and 12.5 ppm were assigned to Al-OH-Al bridging hydroxides, aromatic CHs, and COOH groups. Similar signals were observed (Fig. 6) to confirm the same structural elements in the synthesised Al-MOF in this study. ^{1}H-NMR of a zinc-based MOF was provided in [38]. Signals at 7.6 ppm and 47.7 ppm said to indicate the interactions between the metal atoms and aromatic hydrogens of terephthalic group. In present study, Zn-MOF was synthesised with furandicarboxylic acid linkers, and strong signals at around 0.5 and 5.0 ppm were observed. These indicate presence of some hydrogens between the building blocks. ZIF-8 MOF was studied [39], and signals at 7.0 and 2.1 ppm corresponding CH-groups in the imidazole ring and the methyl group were identified. In this study (Fig. 6), signals at -1.2 ppm and 4.0 ppm were observed for the ZIF-8-MOF synthesised. These signals could only indicate the presence of some hydrogens within the structure. Since C and metal atoms NMRs were not completed in this study, limited evaluations based on hydrogen NMR was possible. The goal of this study was to prove that laboratory synthesised MOFs could be effective adsorbent materials for edible oil refining and purification applications, but not full structural evaluations of the MOFs synthesised. Generally, presence of various hydrogen atoms within all adsorbents were observed at around 0 and 1.0 ppm signals by the ^{1}H NMR.

THERMAL PROPERTIES OF THE ADSORBENTS

Thermal decomposition kinetics of MOFs were usually determined with thermal gravimetric analysis (TGA) [3, 8, 18]. It was shown that a mass decrease for MIL-53 at around 300°C occurred, which was attributed to the decomposition of MOF crystals according to the sharp endothermic peak at around 580°C [3]. Similarly, TGA indicated that thermal degradation of Zn-MOF and Ti-MOF starts at temperatures above 410°C, while it was above 500°C for Al-MOF sample [8]. In this study, the aim of differential scanning calorimetry analysis was to observe any possible thermal phase transitions rather than decompositions since the main goal of this study was to determine the possible suitability of the synthesised MOFs for edible oil purification applications. In edible oil industry, adsorbents were used at temperatures never exceeding 200°C. Hence, a DSC analysis was enough for the purpose. Thermal analysis with DSC from 30 to 450°C was completed, and the findings were presented in Table III.

These data give phase changes and limited thermal stability clues. There were no observable peaks for Ti-MOF and C.B.E. samples. There were two endothermic peaks at 256.07 and 316.91°C for the γ-CD-MOF sample. These peaks indicate a possible decomposition of γ-CD-MOF at that temperatures. In fact, among all the adsorbents studied, only the γ-CD-MOF included organic materials, namely the

Table III - The thermal properties of the MOFs and natural clays

	Onset (°C)	End (°C)	Peak (°C)	ΔH (J/g)
Ti-MOF	-	-	-	-
γ-CD-MOF	29.01	147.35	88.02	205.2696
γ-CD-MOF Fraction 2	247.47	259.42	256.07	-25.1746
γ-CD-MOF Fraction 3	299.68	334.98	316.91	-50.0621
Cr-MOF	343.52	385.86	372.47	93.875
Al-MOF	39.34	99.92	84.15	109.6877
Zn-MOF	261.7	283.25	272.98	19.2049
Mg-MOF	290.83	302.62	298.06	26.0635
ZIF-8-MOF	375.72	412.43	396.29	14.2121
C.B.E.	-	-	-	-
Zeolite	41.19	131.34	81.81	94.9526
Sepiolite	35.37	109.32	71.38	99.4164

gamma-cyclodextrine, within its mass. Hence, at temperatures above 250°C, decomposition of gamma-cyclodextrine may have occurred. Thus, applications of the γ-CD-MOF must be below 200°C for the thermal stability of the structure. Since in oil industry, applications are usually well below 150°C, there would be no problem arising. Other exothermic peak at around 100-120°C for the MOFs (Tab. III) might probably for the phase transitions of the water molecules trapped within the frames. Rest of the exothermic peaks were ranged from the lowest of 71.38°C for sepiolite to the highest of 396.29°C for the ZIF-8-MOF, respectively (Tab. III). Mu and Watson [40] studied thermal properties of 9 different MOF samples. DSC determined end temperatures for the samples ranged between 175.7 and 321.4°C. Also, thermal stability temperatures were measured between 285 and 560°C. Generally, DSC data in this study and their findings concur. Overall, except γ-CD-MOF, all adsorbents were found quite stable up to 450°C, and γ-CD-MOF must be used below 200°C for thermal stability. Since adsorbent applications in edible oil industry (decolorization, physical refining, oil regeneration, flavour correction, removal of turbidity etc.) take place below 150°C, the MOFs synthesised in this study could be suitably used.

FREE FATTY ACID AND β-CAROTENE ADSORPTION CAPACITY OF THE ADSORBENTS

As the most important adsorbent properties for edible oil purification applications, the free fatty acid (FFA) and β-carotene (β-CA) adsorption capacities of the adsorbents were determined, and the results were presented in Table IV.

Although statistically there was no difference among the Ti-MOF, γ-CD-MOF, Cr-MOF, Mg-MOF, ZIF-8-MOF, and sepiolite for the FFA adsorption capacity, the measured highest value was 16.03 mg oleic acid/g adsorbent for Ti-MOF. Contrarily, zeolite (4.50 mg oleic acid/g) and C.B.E. (5.72 mg oleic acid/g) had the lowest values. Clearly, Ti-MOF had more than 3-fold higher adsorption capacity than the commercial bleaching earth (C.B.E.) for the FFAs. This is a very significant result putting the advantegeous ability of the MOFs. Similarly, the highest β-CA adsorption capacity (168.92 μg β-carotene/g adsorbent) was measured in Ti-MOF sample. This value was still higher than that of the C.B.E. (153.75 μg β-carotene/g adsorbent). The γ-CD-MOF and sepiolite had values

Table IV - The free fatty acid and carotene adsorption capacities of the MOFs and natural clays

	Free Fatty Acid Adsorption Capacity (mg Oleic acid/g)	Carotene Adsorption Capacity (μg β-Caroten/g)
Ti-MOF	16.03±1.7^{a}	168.92±6.9^{a}
γ-CD-MOF	15.80±2.1^{a}	152.35±7.1^{b}
Cr-MOF	14.90±1.3^{a}	75.50±5.0^{e}
Al-MOF	8.60±2.7^{b}	82.90±7.5^{d}
Zn-MOF	7.03±3.5^{b}	100.20±5.9^{c}
Mg-MOF	13.89±2.1^{a}	74.10±3.9^{e}
ZIF-8-MOF	14.92±1.5^{a}	73.90±4.7^{e}
C.B.E.	5.72±1.0^{c}	153.75±3.2^{b}
Zeolite	4.50±1.2^{c}	89.30±10.2^{c,d}
Sepiolite	14.05±2.1^{a}	150.05±7.3^{b}

*Small uppercase letters in the same columns show statistically significant differences among the adsorbent materials ($p \leq 0.05$).

near C.B.E. as well. Furthermore, these adsorption treatments were carried out at ambient temperature. In edible oil industry, bleaching operation was carried out by adding around 0.15-3.0% of commercial clays into oil, and then heating oil to around 105-110°C meanwhile mixing for at least half an hour before filtration. Most of the time bleaching was done under vacuum and hermetic conditions to prevent oil oxidation in expense of extra cost. By industrial bleaching, most color pigments (carotenes and chlorophyll), residual soaps, peroxides, trace metals, remaining phospholipids, aldehydes and ketones, and other impurities are removed [9]. Hence, bleaching is an indispensable part of edible oil refining. Clearly, Ti-MOF at first, and then γ-CD-MOF showed significantly higher adsorption capacities at ambient temperature. Hence, adaptation of these materials for edible oil bleaching could provide significant advantages.

In industrial applications, adsorption temperature, time and adsorbent addition level would be important parameters. Although in this study only one adsorbent addition level and one treatment temperature were used, Sabah et al [41] used different adsorbent dosages and treatment temperatures to decolorise vegetable oils with activated sepiolite. In the same study [41], Langmuir and Freundlich models together with mass-balance equation were used to calculate the kinetic parameters. The equations are given below [41] and would be used for similar purposes with further studies for MOFs as adsorbents.

Langmuir model: $C_e / X = [(1 / K_L X_m) + (1 / X_m)] C_e$

Freundlich model: $X = K_F C_e^{1/n}$

Mass-balance: $X = [(C_o - C_e) V / 1000m]$

Where, C_e is the equilibrium concentration of β-CA or FFA, X is the amount of β-CA or FFA adsorbed per gram of the adsorbent, C_o is the initial concentration of β-CA or FFA, X_m is the quantity of β-CA or FFA adsorbed at monolayer or maximum coverage, K_L is the Langmuir equilibrium constant, K_F is the Freundlich equilibrium constant, m is the mass of the adsorbent, and V is the mass of the oil.

Furthermore, adsorbents have not only been applied for bleaching purpose in edible oil industries, but also, they have been applied as aid materials for physical refining [11] and regeneration of used frying oils [13], as filter aids for turbidity removal and clearance [13], and other purposes.

In the present study, 7 different MOFs were selected based on their safety data to apply in food processing and synthesised in laboratory at gram levels for further analysis. Although MOF leaching study was not carried out in this study, previous studies [7, 8] indicated that MOFs are fairly stable structures and no metal leakage occurs into the oil. In addition, 3 natural clays (commercial bleaching earth, natural zeolite and sepiolite) included in this study. The main purpose was to evaluate the adsorbent properties of the materials for possible applications in edible oil industries. Surface properties revealed that, Al-MOF and ZIF-8-MOF had significantly higher surface areas, while largest pore volumes were present in sepiolite and Ti-MOF samples. Likewise, γ-CD-MOF, Zn-MOF and Ti-MOF had the largest pore radia. Microstructures of the adsorbents were evaluated by SEM images and X-RD patterns indicated that crystals with various geometrical morphologies and crystalline forms were formed. The NIR and solid ^{1}H NMR spectra indicated that these MOFs present various structural elements with hydrogen atoms located around metal nuclei, proving the X-RD patterns. Thermal analysis completed with DSC indicated that except γ-CD-MOF, all are quite heat stable up to 450°C. For γ-CD-MOF, working temperatures not exceeding 200°C is suggested. Most importantly, especially Ti-MOF, γ-CD-MOF and Cr-MOF were shown to have higher adsorption capacities for FFA and β-CA. Overall, results of this study pointed out that the studied MOFs have a very huge potential to apply them in edible oil purification studies. Research involving applications of these MOFs in crude oil refining and decolorization, regeneration of used frying oils, aroma (odor) corrections of fish oil, bitterness removal from oils, and others have been in progress in our laboratory, and the findings will duly be presented in future articles.

Acknowledgements

This study was funded by the TUBITAK (The Scientific and Technological Research Council of Turkey) with Project No: 215O348. The authors thank for the support. We also thank Trakya Birlik Oil Processing Factory (Çorlu, Tekirdağ), Rota Mines Co. (İstanbul), and Madkim Coal and Chem. Co. (İstanbul) for gifting us the commercial bleaching earth, natural zeolite and sepiolite.

BIBLIOGRAPHY

[1] N. Stock, S. Biswas. Synthesis of metal-organic frameworks (MOFs): routes to various MOF topologies, morphologies, and composites. Chem. Rev. *112*(2) 933-969, (2012)

[2] H. Furukawa, K. Cordova, M. Keeffe, O. Yaghi. The chemistry and applications of metal-organic frameworks. Science *341*(6149), 123-444 (2013)

[3] Y. Ma, J. Lin, Y. Xue, J. Li, Y. Huang, C. Tang. Acid-assisted hydro thermal synthesis and adsorption properties of high-specific-surface metal-organic frameworks. Materials Letters *132*, 90-93 (2014)

[4] C. Dey, T. Kundu, B.P Biswal, A. Mallick, R. Ba-

nerjee. Crystalline metal-organic frameworks (MOFs): synthesis, structure and function. Acta Crystallographica Section B *70*, 3-10 (2014)
[5] A. Czaja, E. Leung, N. Trukhan, U. Müller. Industrial MOF synthesis. In: Farruseng, D. (ed.) Metal-Organic Frameworks: Application from Catalysis to Gas Storage, pp. 339. Wiley-VCH, New York (2011)
[6] R.A. Smaldone, R.S Fogan, H. Furukawa, J.J Gassemith, A.M.Z. Slawin, O.M. Yaghi. Metal-organic frameworks from edible natural products. Angewandte Chemie International Edition, 49-8630 (2010)
[7] N. Li, L. Zhang, L. Nian, B. Cao, Z. Wang, L. Lei, X. Yang, J. Sui, H. Zhang, A. Yu. Dispersive micro-solid-phase extraction of herbicides in vegetable oil with metal-organic framework MIL-101. Journal of Agricultural and Food Chemistry *63*, 2154-2161 (2015)
[8] E.A. Vlasova, S.A. Yakimov, E.V. Naidenko, E.V. Kudrik, S.V. Makarov. Application of metal-organic frameworks for purification of vegetable oils. Food Chemistry *190*, 103-109 (2016)
[9] A.S. Hodgson. Refining and bleaching. In: Hui, Y. H. (ed.) Bailey's Industrial Oil and Fat Products 157-212. Wiley-Interscience, New York (1996)
[10] E. Sabah, M. Çinar, M.S. Çelik. Decolorization of vegetable oils: Adsorption mechanism of β-carotene on acid-activated sepiolite. Food Chemistry *100*(4), 1661–1668. (2007)
[11] D. Anderson. A Primer on oils processing technology. In: Bailey's Hui, Y. H. (ed.) Industrial Oil and Fat Products, 1-60. Wiley-Interscience, New York (1996)
[12] J. Huang, S. Sathivel. Purifying salmon oil using adsorption, neutralization, and a combined neutralization and adsorption process. Journal of Food Engineering *96*, 51-58 (2010)
[13] A. Dülger, E. Yılmaz. Effectiveness of modified zeolites as adsorbent materials for frying oils. European Journal of Lipid Science and Technology 115, 668-675 (2013)
[14] R.D. O'Brien, Fats and Oils: Formulating and Processing for Applications. New York, US (2004)
[15] Z. Moussa, M. Hmadeh, M.G. Abiad, O.H. Dib, D. Patra. Encapsulation of curcumin in cycodextrin-metal organic frameworks: Dissociation of loaded CD-MOFs enhances stability of curcumin. Food Chemistry *212*, 485-494 (2016)
[16] F. Bu, Q. Lin, Q Zhai, L. Wang, T. Wu, S-T. Zheng, X. Bu, P. Feng. Two zeolite-type frameworks in one metal-organic framework with Zn24@Zn104 cube-in-sodalite architecture. Angewandte Chemie International Edition *51*, 8538-8541 (2012)
[17] I. Spanopoulos, I. Bratsos, C. Tampaxis, A. Kourtellaris, A. Tasiopoulos, G. Charalambopoulou, T.A. Steriotis, P.N. Trikalitis. Enhanced gas-sorption properties of a high surface area, ultra micro porous magnesium formate. CrystEngComm *17*, 532-539 (2015)
[18] K.S. Park, Z. Ni, A.P. Cote, J.Y. Choi, R. Huang, F.J Uribe-Romo, H.K. Chae, M. O'Keeffe, O. Yaghi. Exceptional chemical and thermal stability of zeolitic ımidazolate frameworks. Proceedings of the National Academy of Sciences of the United States of America *103*(27), 10186-10191 (2006)
[19] P. Peerajit, N. Chiewchan, S. Devahastin. Effects of pretreatment methods on health-related functional properties of high dietary fibre powder from lime residues. Food Chemistry *132*, 1891-1898 (2012)
[20] L. Ngamwonglumlert, S. Devahastin, N. Chiewchan. Effects of pretreatment and drying methods on molecular structure, functional properties and thermal stability of fibre powder exhibiting colour from *Centella asiatica* L. International Journal of Food Science & Technology *51*, 753-764 (2016)
[21] D.S. Ferraira, R.J. Poppi, J.A.L Pallone. Evaluation of dietary fiber of Brazilian soybean (Glycine max) using near-infrared spectroscopy and chemometrics. Journal of Cereal Science *64*, 43-47 (2015)
[22] O.O. Taspınar, S. Özgül-Yücel. Lipid adsorption capacities of magnesium silicate and activated carbon prepared from the same rice hull. European Journal of Lipid Science and Technology *110*, 742-746 (2008)
[23] D.B. Rodriguez-Amaya, M. Kimura. HarvestPlus Handbook for Carotenoid Analysis. HarvestPlus, Washington (2004)
[24] Minitab. Minitab Statistical Software (Version 16.1.1). Minitab Inc., State College, Pennsylvania (2010)
[25] SPSS. SPSS Professional Statistics (Version 10,1). SPSS Inc., Chicago (1994)
[26] H.J. Lee, J. We, J.O. Kim, D. Kim, W. Cha, E. Lee, J. Sohn, M. Oh. Morphological and structural evolutions of metal-organic framework particles from amorphous spheres to crystalline hexagonal rods. Angewandte Chemie International Edition *54*, 10564-10568 (2015)
[27] S. Naeimi, H. Faghihian. Performance of novel adsorbent prepared by magnetic metal-organic framework (MOF) modified by potassium nickel hexacyanoferrate for removal of Cs± from aqueous solution. Separation and Purification Technology *175*, 255-265 (2017)
[28] S. Granick, N. Yanai, M. Sindoro, A.Y. Jee. Colloidal-sized metal-organic frameworks: synthesis and applications. Accounts of Chemical Research *47*(2), 459-469 (2013)

[29] S. Kitagawa, S. Horike. Design of porous coordination polymers/metal–organic frameworks: past, present and future. In: Farrusseng, D. (ed.) Metal-Organic Frameworks, 1-19. Wiley-VCH, Fransa (2011)
[30] W. Cho, H.J. Lee, M. Oh. Growth-controlled formation of porous coordination polymer particles. Journal of the American Chemical Society *130*(50), 16943-16946 (2008)
[31] D.A. Skoog, J.J. Leary. Infrared absorption spectroscopy. In: Fouth (ed.) Principles of Instrumental Analysis, pp. 252. Saunders College Pub., New York (1992)
[32] Y-P. Wang, X-Y. Li, H-H. Li, H-Z. Zhang, H-Y. Sun, Q. Guo, H. Li, Z. Niu. A novel 3D Nd(III) metal-organic frameworks based on furan-2,5-dicarboxylic acid exhibits new topology and rare near-infrared luminescence property. Inorganic Chemistry Communications *70*, 27-30 (2016)
[33] J. Ethiraj, F. Bonino, C. Lamberti, S. Bordiga. H_2S interaction with HKUST-1 and ZIF-8 MOFs: A multitechnique study. Microporous and Mesoporous Materials *207*, 90-94 (2015)
[34] A. Sutrisno, Y. Huang. Solid-state NMR: A powerful tool for characterization of metal-organic frameworks. Solid State Nuclear Magnetic Resonance *49-50*, 1-11 (2013)
[35] A.J. Rossini, A. Zagdoun, M. Lelli, J. Canivet, S. Aguado, O. Ouari, P. Tordo, M. Rosay, W.E. Maas, C. Coperet, D. Farrusseng, L. Emsley, A. Lesage. Dynamic nuclear polarization enhanced solid-state NMR spectroscopy of functionalized metal-organic frameworks. Angewandte Chemie International Edition *124*, 127-131 (2012)
[36] M. Haouas, C. Volkringer, T. Loiseau, G. Ferey, F. Taulelle. The Extra-Framework Sub-Lattice of the Metal–Organic Framework MIL-110: A Solid-State NMR Investigation. Chemistry – A European Journal *15*, 3139-3146 (2009)
[37] T. Loiseau, C. Serre, C. Huguenard, G. Fink, F. Taulelle, M. Henry, T. Bataille, G.A. Ferey. Rationale for the Large Breathing of the Porous Aluminum Terephthalate (MIL-53) Upon Hydration. Chemistry – A European Journal *10*, 1373-1382 (2004)
[38] T. Uemura, S. Horike, K. Kitagawa, M. Mizuno, K. Endo, S. Bracco, A. Comotti, P. Sozzani, M. Nagaoka, S. Kitagawa. Conformation and molecular dynamics of single polystyrene chain confined in coordination nanospace. Journal of the American Chemical Society *130*, 6781-6788 (2008)
[39] C. Chmelik, D. Freude, H. Bux, J. Haase. Ethene/ethane mixture diffusion in the MOF sieve ZIF-8 studied by MAS PFG NMR diffusometry. Microporous and Mesoporous Materials *147*, 135-141 (2012)
[40] B. Mu, K.S. Watson. Thermal analysis and heat capacity study of metal organic frameworks. The Journal of Physical Chemistry C *115*, 22748-22754 (2011)
[41] E. Sabah, M. Çinar, M.S. Çelik. Decolorization of vegetable oils: adsorption mechanism of b-carotene on acid-activated sepiolite. Food Chemistry *100*, 1661-1668 (2007)

Received: March 30, 2018
Accepted: August 8, 2018